Published in final edited form as:
Harmful Algae. 2013 June ; 26: 12–19. doi:10.1016/j.hal.2013.03.001.

Brevenal, a brevetoxin antagonist from Karenia brevis, binds to a previously unreported site on mammalian sodium channels

Elena P. Gold[†], **Henry M. Jacocks**[†], **Andrea J. Bourdelais**[†,*], and **Daniel G. Baden**[†]
[†]Center for Marine Science, University of North Carolina at Wilmington, 5600 Marvin K. Moss Lane, Wilmington, North Carolina 28409

Abstract

Brevetoxins are a family of ladder-frame polyether toxins produced by the marine dinoflagellate *Karenia brevis*. During blooms of *K. brevis*, inhalation of brevetoxins aerosolized by wind and wave action can lead to asthma-like symptoms in persons at the beach. Consumption of either shellfish or finfish contaminated by *K. brevis* blooms can lead to the development of neurotoxic shellfish poisoning. The toxic effects of brevetoxins are due to binding at a defined site on, and subsequent activation of, voltage-sensitive sodium channels (VSSCs) in cell membranes (site 5). In addition to brevetoxins, *K. brevis* produces several other ladder-frame compounds. One of these compounds, brevenal, has been shown to antagonize the effects of brevetoxin. In an effort to further characterize to effects of brevenal, a radioactive analog ([^{3}H]-brevenol) was produced by reducing the side-chain terminal aldehyde moiety of brevenal to an alcohol using tritiated sodium borohydride. A K_D of 67 nM and B_{max} of 7.1 pmol/mg protein were obtained for [^{3}H]-brevenol in rat brain synaptosomes, suggesting a 1:1 matching with VSSCs. Brevenal and brevenol competed for [^{3}H]-brevenol binding with K_i values of 75 nM and 56 nM, respectively. However, although both brevenal and brevenol can inhibit brevetoxin binding, brevetoxin was completely ineffective at competition for [^{3}H]-brevenol binding. After examining other site-specific compounds, it was determined that [^{3}H]-brevenol binds to a site that is distinct from the other known sites including the brevetoxin site (site 5) although some interaction with site 5 is apparent.

Keywords

Brevenal, Brevetoxin; Radioligand Assay; Competition Binding Assay

1. Introduction

The dinoflagellate responsible for Florida red tides, *Karenia brevis* (formerly *Gymnodinium brevi*, formerly *Ptychodiscus brevis*), produces numerous fused-ring polyether compounds, the most abundant of which are the brevetoxins (PbTxs) (Baden and Tomas, 1988). Naturally occurring brevetoxins (Figure 1) comprise a family of compounds distributed between two basic frameworks, PbTx-A and PbTx-B, with the PbTx-B derived compounds generally the more abundant both in culture and in the environment (Baden, 1983; Lin *et al.*, 1981; Shimizu *et al.*, 1986). Brevetoxins are the agents believed to be responsible for massive fish kills and marine mammal poisoning during Florida red tides. In mammals,

[*]Corresponding Author, Tel: 910-962-2365, FAX: 910-962-2410, bourdelaisa@uncw.edu.

consumption of brevetoxin-tainted shellfish has resulted in neurotoxic shellfish poisoning (NSP) (Baden *et. al.*, 1995; Baden and Mende 1982 (humans); Bossart *et al.*, 1998 (manatees); Flewelling *et al.*, 2005 (dophins)). Environmental exposure to aerosolized brevetoxin during Florida red-tides often results in upper respiratory and ocular irritation (Baden, 1983; Steidinger and Baden, 1984; Watanabe *et al.*, 1988; Kirkpatrick *et al.*, 2001; Abraham *et al.*, 2005; Fleming *et al.*, 2005; Fleming *et al.*, 2007; Backer *et al.*, 2003, 2005). The toxic effects of brevetoxins are due, in part, to their ability to bind very selectively to site 5 on voltage-sensitive sodium channels (VSSCs) (Poli *et al.*, 1986) and the deleterious effects of ingestion of brevetoxins (NSP) are likely due primarily to subsequent sustained activation of VSSCs (Purkerson-Parker *et al.*, 2000).

While Purkerson-Parker and colleagues (2000) examined the ability of natural brevetoxins to competitively inhibit the binding of tritiated brevetoxin in rat brain synaptosomes, other fused-ring polyether compounds, including hemibrevitoxin B (Shimizu *et al.*, 1990), brevisin (Satake *et al.*, 2009), brevisamide (Satake *et al.*, 2008), tamulamide A and B (Truxal *et al.*, 2010), brevenal (Bourdelais *et al.*, 2004), brevenol (Baden *et al.*, 2005) and many others, are yet to be fully characterized (Bourdelais *et al.*, unpublished results). Such compounds have been extracted from cultures of *K. brevis* and many have been detected in environmental samples collected during red tides (Pierce *et al.*, 2003). Of the aforementioned group of compounds, brevenal (Figure 2) is of particular interest. Brevenal has been shown to inhibit the binding of brevetoxins to rat brain synaptosome VSSCs, albeit with approximately 100-fold lower affinity than brevetoxins (Bourdelais *et al.*, 2004). Brevenal, at moderate to high concentrations, also appeared to have no toxic effects of its own. However, in the case of exposure to aerosolized brevetoxins in an asthmatic sheep model, brevetoxin induced a concentration-dependent bronchoconstriction which was ameliorated by pretreatment with brevenal, at concentrations of brevenal 100-fold lower than would be expected based on synaptosome binding affinities (Abraham *et al.*, 2005) suggesting that brevenal may be acting on a receptor site different or in concert with the brevetoxin binding site. In fact, in the absence of inhaled toxin, brevenal itself was able to improve airway function (mucociliary clearance) as indicated by increased tracheal mucus velocity (TMV), suggesting an alternative mode of action for brevenal that may be of clinical use in conditions where dysregulation of ionic transport causes decreased mucociliary clearance, such as cystic fibrosis (CF) or COPD. In a comparison study with the sodium channel blocker amiloride (used to increase mucociliary transport in CF patients), brevenal was shown to achieve the same improvement in TMV as amiloride but at a concentration 10^6-fold lower, thus making it a lead compound in the search for more effective therapeutic control of mucociliary diseases such as cystic fibrosis (Potera, 2007).

Like brevetoxins, ciguatoxins are another family of ladder-frame polyethers that are produced by a marine dinoflagellate (*Gambierdiscus toxicus).* Ciguatoxins also selectively bind to VSSC site 5 on the membranes of excitable cells to cause an increase in membrane permeability and excitability (Mattei *et al.*, 1999). Similar to brevetoxins, ciguatoxin is also associated with deleterious health effects in humans and is believed to be the causative agent in the human condition known as ciguatera. Ciguatera is characterized by nausea, vomiting and neurological dysfunction, including a tingling sensation or reversal of temperature perception. As seen with brevetoxins, brevenal also attenuates the effects of ciguatoxin in mammalian tissues. Brevenal was shown to inhibit neurosecretion in bovine chromaffin cells caused by pacific ciguatoxin 1b (P-CTX-1B) (Mattei *et al.*, 2008). Inhibition data for brevenal in the presence of P-CTX-1B treatment were biphasic in nature, showing an initial affinity in the nanomolar range and subsequently, in the micromolar range. This effect was increased when the concentration of P-CTX-1B was increased. Therefore, like the asthmatic sheep assay with brevetoxins, brevenal exhibits an initial antagonism of ciguatoxins at values 100-fold lower than reported for synaptosome binding assays but similar to values for

antagonism of brevetoxins. Because of the peculiar dichotomy between extant binding data and efficacy as an antitoxin, it is believed that brevenal may be influencing sites other than site 5 of the VSSC's. In order to determine if brevenal was acting on sites other than the brevetoxin binding sites it was decided to produce a more selective marker (other than ^{3}H-PbTx-3) to help elucidate the mechanism of action of brevenal. Prior studies using [^{3}H]-PbTx-3, produced by reduction of the aldehyde side chain of PbTx-2 with $NaB^{3}H_4$, revealed that, at least for brevetoxin binding, relatively minor changes (from an aldehyde to an alcohol) in the side chain cause minimal changes in binding characteristics between PbTx-2 (aldehyde) and PbTx-3 (alcohol) with inhibition constants (K_i) of 0.81 nM and 1.6 nM, respectively (prior published values range from 0.5 - 3 nM). Since brevenal is a fused-ring polyether system with a terminal aldehyde moiety, similar to brevetoxin, a tritiated alcohol derivative of brevenal was the natural choice for the development of a radioligand for the characterization of the brevenal binding site in rat brain synaptosomes. Synthesis of the tritiated derivative was successful and binding studies with tritiated brevenol ([^{3}H]-brevenol) (Figure 2) were initiated.

2. Materials and Methods

2.1 Materials

Brevenal, PbTx-2 and PbTx-3 were purified from unialgal cultures of *Karenia brevis* (Wilson strain) as previously described in Bourdelais *et al.*, (2004). Tritiated sodium borohydride ($NaB^{3}H_4$: 80 Ci/mmol) was purchased from American Radiolabeled Chemicals, Inc. (St. Louis, MO). All other compounds were reagent grade or better and were obtained from commercial sources. Frozen whole rat brains (adult male; Sprague-Dawley) were purchased from Harlan (Indianapolis, IN). ^{3}H-PbTx-3 was produced from PbTx-2 as described in Poli *et al.* (1985).

2.2 Preparation and Characterization of Brevenol and Tritiated Brevenol ([^{3}H]-brevenol)

Brevenol was prepared by the reduction of the aldehyde function on brevenal to an alcohol using $NaBH_4$ (Figure 2). All solvents were dried over molecular sieves before use. $NaBH_4$ was dissolved in dimethylformamide (DMF) (0.4 M) and added to a reaction vessel containing brevenal in methanol and a thirty-fold molar excess of cerium chloride. The reaction was performed at room temperature with constant stirring. The reaction was quenched by the addition of acetone. The synthesis of [^{3}H]-brevenol paralleled the synthesis of the unlabeled form of this molecule, substituting $NaB^{3}H_4$ for $NaBH_4$.

The product mixture was partitioned between diethyl ether and distilled water. The ether layer was dried and then dissolved in MeOH for further purification by high performance liquid chromatography (HPLC). Initial separation (Phenomenex Luna 5 ! m C18 250 mm × 4.6 mm; mobile phase 90% MeOH/10% H_2O at 1.4 mL/min; UV detection at 215 nm) yielded two major groups of peaks. Subsequent separation of both groups on a different column (Phenomenex Luna 5 mm phenyl hexyl, 250 mm × 4.6 mm; mobile phase and detection as above) yielded multiple peaks, one of which (t_r = 4 min) was determined to be brevenol by NMR using 1-D and 2-D experiments (Bruker 500 MHz NMR;5.0 mm TXI probe: ^{1}H, ^{13}C, ^{1}H-^{13}C HMBC, ^{1}H-^{13}C HSQC, ^{1}H COSY and ^{1}H ROESY).

The purification of the reduction reaction product of brevenal to [^{3}H]-brevenol closely resembled the protocol for the unlabeled reduction previously described. The labile tritium atom attached to the alcohol oxygen was removed by multiple extractions in ethyl ether/H_2O and subsequent HPLC procedures. However, [^{3}H]-brevenol purification and identification was conducted based on the HPLC retention times of brevenol (unlabeled) because the NMR spectrometer was not available for use with tritiated materials. In order to determine

the identity of [^{3}H]-brevenol, retention times on the C18 and phenyl hexyl columns were compared and brevenol (non-radioactive) was mixed with putative [^{3}H]-brevenol and analyzed by HPLC (C18 column and conditions as above). Brevenol and [^{3}H]-brevenol eluted as a single peak.

2.3 Preparation of Synaptosomes

The preparation of synaptosomes was modified from Dodd *et al.* (1981) as described in Poli *et al.* (1985). All equipment in contact with the brains/homogenates was at ice temperature. Ten frozen rat brains were thawed on ice and homogenized in 10 mL of ice-cold homogenization buffer (0.32 M sucrose, 0.005 M sodium phosphate and a protease inhibitor cocktail of 1 mM iodoacetamide, 0.1 mM PMSF, 1 mM, 1:10 phenanthroline and 1 ! M pepstatin A brought to pH 7.4 with H_3PO_4) with ten excursions of a motor driven Teflon/glass homogenizer. The resulting homogenate was sedimented at 700 × g for 10 min at 4 °C. The supernatant was saved and the pellet was resuspended in 10 mL homogenization buffer and homogenized again. Sedimentation was repeated at 700 × g as above. The second supernatant was combined with the first and the pellet was discarded. The supernatant mixture was layered over 3 mL of 1.2 M sucrose solution (containing protease inhibitors included in the homogenization buffer) in 10 mL polyallomer centrifuge tubes and centrifuged at 105,000 × g for 30 min at 4 !C. The material at the interface, between the 0.32 M and 1.2 M sucrose solutions, was collected, minimizing the amount of 1.2 M sucrose solution included. The material was diluted with homogenization buffer, layered over 0.8 M sucrose solution (containing protease inhibitors) in 5 mL polyallomer centrifuge tubes and centrifuged at 140,000 × g for 35 min at 4 !C. The final pellet containing synaptosomes was resuspended by trituration in standard binding medium (SBM) (50 mM HEPES, 130 mM choline chloride, 5.4 mM KCl, 0.8 mM magnesium sulfate, 5.5 mM glucose, 1mM EGTA and the protease inhibitor cocktail previously listed for the homogenization buffer brought to pH 7.4 with Tris base). In a departure from the original protocol, detergent was not added to the SBM in order to decrease non-specific radioligand binding. The resulting suspension was diluted to 1 mg protein/mL and aliquots were stored at ⁻80 °C for use in subsequent assays.

2.4 Radioligand binding

Binding of [^{3}H]-PbTx-3 and [^{3}H]-brevenol to rat brain synaptosomes was measured independently using a rapid centrifugation technique as described by Poli *et al.* (1985). All buffers, reagents, and plastic ware were at ice temperature throughout each experiment except during centrifugation (see below). All experiments were performed in SBM with 1 mg/mL bovine serum albumin (BSA) (SBM + BSA) without detergent.

2.5 Saturation binding

Total binding (specific + non-specific) was determined as follows. A stock solution of radiolabeled probe ([^{3}H]-PbTx-3: ≈100 nM or [^{3}H]-brevenol: ≈3 ! M) was prepared in SBM +BSA and serially diluted (1:2) in SBM+BSA to below 1 nM. Synaptosomes (50 ! L) were added to Eppendorf tubes containing SBM+BSA (395 ! L) and reagent alcohol (5 ! L) and allowed to stand for 30 min. Radioligand (50 ! L) was added (triplicates at each dilution); the tubes were vortexed and were allowed to stand for 30 min. Tubes were centrifuged for 2 min. at 14,000 × g. The supernatants were rapidly aspirated and the pellet quickly washed with 2-3 drops of ice-cold wash medium (163 mM choline chloride, 5 mM HEPES, 1.8 mM calcium chloride, 0.8 mM magnesium sulfate, 1 mg/mL BSA brought to a pH of 7.4 using Tris base). The pellets were transferred to scintillation vials, suspended in 2.5 mL Scintiverse biodegradable scintillation fluid (Fisher Scientific), and allowed to stand overnight. The samples were vortexed immediately before measuring radioactivity. The

bound radioactivity was determined by liquid scintillation spectrometry using the LS 6500 Liquid Scintillation Counter (Beckman Coulter; Brea, CA).

Non-specific binding was determined at the same time as the total binding using a parallel set of Eppendorf tubes with the same contents and procedures with the exception being replacement of the reagent alcohol with a reagent alcohol solution of PbTx-2 (1 mM) when using [^{3}H]-PbTx-3 or brevenal or brevenol (5 mM) for [^{3}H]-brevenol. Specific binding was calculated as the difference between total binding and nonspecific binding at each concentration of radioligand. The specific binding curves were analyzed by non-linear regression analysis by GraphPad Prism version 4.0 for Windows, GraphPad Software, San Diego California USA, www.graphpad.com to yield equilibrium dissociation constants (K_D) and binding maxima (B_{max}) and to compare the fit of the data to one-site and two-site models using the extra sum-of-squares F test. K_D and B_{max} values obtained with brevenol as the unlabeled ligand were compared to values obtained with brevenal as the unlabeled ligand using an unpaired Student's t-test (two-tailed) in GraphPad Prism 4.0.

2.6 Inhibition of binding

The inhibition of binding of each radiolabeled ligand was determined in the presence of various competitors (ranging in concentration from 10^{-12} M to 10^{-5} M (or 5×10^{-6} to 50 mg/mL). In these experiments, the radioligand concentration was fixed (≈3 nM for [^{3}H]-PbTx-3 and ≈9 nM for [^{3}H]-brevenol, final concentrations) and serial dilutions of the unlabeled competitor were prepared in reagent alcohol. Otherwise, the protocol was the same as for saturation binding (*i.e.* incubation of synaptosomes with each dilution of unlabeled competitor for 30 min. followed by addition of radioligand and an additional 30 min incubation prior to centrifugation). Equilibrium inhibition constants (K_i) were determined by non-linear regression analysis by GraphPad Prism version 4.00 for Windows, GraphPad Software, San Diego California USA, www.graphpad.com.

For double reciprocal (*i.e.* Lineweaver-Burk) analyses (*i.e.* 1/bound vs. 1/free), both the unlabeled and labeled ligand concentrations were varied, as indicated. "Bound" label was considered to be the values obtained from the pellet and "free" was determined by taking an aliquot from the supernatant after centrifugation and correcting for volume..

3. Results

In detergent-free medium, saturation binding analyses yielded values for [^{3}H]-PbTx-3 binding (K_D = 2.6 nM; B_{max} = 7.1 pmol/mg protein) that were similar to those obtained in studies where detergent was present in the medium. The extra sum-of-squares F test performed on the specific binding data rejected the two-site model because the data fit the one-site model better. Concentration-dependent inhibition of [^{3}H]-PbTx-3 binding was observed for PbTx-2 and PbTx-3 (Figure 3) with K_i values (0.81 nM and 1.6 nM, respectively) similar to the range of values previously reported (0.5 nM to 3 nM respectively). Brevenal and brevenol also inhibited [^{3}H]-PbTx-3 binding in a concentration-dependent manner with K_i values of 98 nM and 661 nM, respectively. Double reciprocal analysis of PbTx-2, PbTx-3 (Poli, 1986), brevenal (Bourdelais *et al.*, 2004) and brevenol (Figure 4) inhibition of [^{3}H]-PbTx-3 binding generated data plots which converge near the ordinate, suggesting competitive (versus non-competitive) binding.

Analysis of data from saturation binding experiments revealed that binding (total) of [^{3}H]-brevenol (Figure 5) was concentration-dependent and non-linear. Non-specific binding was concentration-dependent and linear. Subtraction of non-specific binding revealed a saturable specific binding component. Non-linear regression analysis of the specific binding component indicated that [^{3}H]-brevenol binds to rat brain synaptosomes with a K_D of 67 nM

and a B_{max} of 7.1 pmol/mg protein. The two-site model was rejected ($P > 0.05$), implying one-site specific binding. In a subset of saturation experiments performed in parallel, the K_D (69.3 ± 12 nM) and B_{max} (7.0 ± 1.3 pmol/mg protein) values obtained using brevenal to determine non-specific binding were not statistically different ($P > 0.05$) from values obtained using brevenol (K_D = 66.4 ± 5.6 nM; B_{max} = 7.2 ± 0.9 pmol/mg protein) to determine non-specific binding.

Although brevenal and brevenol completely inhibited specific binding (Figure 6) of [^{3}H]-brevenol (with K_i values of 75 nM and 56 nM, respectively), neither PbTx-2 nor PbTx-3 (up to 100 ! M) were able to inhibit [^{3}H]-brevenol binding. Double reciprocal analysis of brevenal and brevenol inhibition of [^{3}H]-brevenol binding (Figure 7) generated data plots which converge near the origin, making it unclear if the interaction is competitive or non-competitive.

Furthermore, In order to further elucidate the nature of the brevenal site, a series of inhibition binding experiments were performed using [^{3}H]-brevenol versus other VSSC site-specific ligands. The results of these studies, summarized in Table 1, reveal that no other site-specific ligands for VSSC's tested were able to inhibit [^{3}H]-brevenol binding to the brevenal site

4. Discussion

Determination of binding characteristics of amphipathic molecules using typical techniques often involves the inclusion of a small amount of detergent to prevent the formation of micelles. In the course of the present studies, it was determined that the non-ionic detergent used (Alkamuls EL) as well as other non-ionic, anionic and cationic detergents tested (data not shown) were a significant source of non-specific binding of [^{3}H]-brevenol. In an effort to minimize the amount of "noise" in the binding signal, the effects of removal of detergent were examined. Binding data obtained for [^{3}H]-PbTx-3 in medium containing detergent did not differ significantly from data obtained with detergent present. These data indicate that the absence of detergent from the binding media does not appear to have significantly compromised the assay and was considered sufficient justification to perform subsequent assays in detergent-free media.

Analysis of data from saturation binding experiments revealed that binding (total) of [^{3}H]-brevenol (Figure 5) was concentration-dependent and non-linear. Non-specific binding was concentration-dependent and linear. Subtraction of non-specific binding revealed a saturable specific binding component. Non-linear regression analysis of the specific binding component indicated that [^{3}H]-brevenol binds to rat brain synaptosomes with a K_D of 67 nM and a B_{max} of 7.1 pmol/mg protein. The two-site model was rejected because theP value obtained was > 0.05), implying one-site specific binding. In a subset of saturation experiments performed in parallel, the K_D (69.3 ± 12 nM) and B_{max} (7.0 ± 1.3 pmol/mg protein) values obtained using brevenal to determine non-specific binding were not statistically different ($P > 0.05$) from values obtained using brevenol (K_D = 66.4 ± 5.6 nM; B_{max} = 7.2 ± 0.9 pmol/mg protein) to determine non-specific binding, consistent with the brevenol binding site being the same as the brevenal binding site. Double reciprocal analysis of PbTx-2, PbTx-3 (Poli, 1986), brevenal (Bourdelais *et al.*, 2004) and brevenol (Figure 4) inhibition of [^{3}H]-PbTx-3 binding generated data plots which converge near the ordinate, suggesting competitive (versus non-competitive) binding. (Uncompetitive inhibition would produce plots that do not converge.)

Because brevenal and brevenol were able to completely inhibit specific [^{3}H]-PbTx-3 binding and because [^{3}H]-PbTx-3 binds selectively to site 5 of VSSCs, it was assumed that brevenal

and brevenol were simply two additional site 5 ligands. However, binding experiments using [^{3}H]-brevenol revealed an interesting dichotomy (Figure 6). Neither PbTx-2 nor PbTx-3 (up to 100 ! M) were able to inhibit [^{3}H]-brevenol binding. These results suggest that [^{3}H]-brevenol and, by inference, brevenal, bind to a site (*i.e.* the "brevenal site") distinct from site 5 on VSSCs. Because brevenal and brevenol can completely inhibit [^{3}H]-PbTx-3 specific binding, the brevenal site is obviously associated with site 5 in some manner. Double reciprocal analysis of brevenal and brevenol inhibition of [^{3}H]-brevenol binding (Figure 7) generated data plots which converge near the origin, making it unclear if the convergence was at the ordinate (implying competitive binding) or at the abscissa (implying non-competitive binding).

Coincidently, published values (6-13.5 pmol/mg protein, Poli *et al.*, 1986) for the B_{max} of [^{3}H]-PbTx-3 within rat brain synaptosomal preparations are similar to the values we obtained for [^{3}H]-brevenol implying a 1:1 binding stoichiometry. Explanations for this binding pattern are dependent on the close proximity of the brevenal/ol receptor to the brevetoxin site (essentially equal in concentration in synaptosomes). Since mutual exclusion of both brevetoxins and brevenal/ol from both receptor sites does not occur, a simple competitive model does not exist. In conclusion, a model in which one ligand (brevenal) and its derivatives sterically hinders the binding of another ligand (brevetoxin) from its site but the reverse is untrue would best explain this binding pattern (much like the pattern illustrated in model 2 of Figure 8 which is adapted from Segel's (1968) models of competitive inhibition of enzyme receptors).

Inhibition of [^{3}H]-brevenol was attempted using ligands selective for other known sites on VSSC. Ligands selective for other known sites were equally ineffective at inhibiting [^{3}H]-brevenol binding as were the brevetoxins. It is well established that there exist allosteric interactions among the different binding sites on VSSCs (Trainer *et al.*, 1993; Cestele and Catterall, 2000; LePage *et al.*, 2003). Future planned studies will address the possibility of allosteric interactions among the identified binding sites and the brevenal site, but the lack of inhibition of [^{3}H]-brevenol binding by ligands selective for these identified sites strongly suggests that the brevenal site is a site distinct from the other known sites on rat brain VSSCs. The high affinity and low non-specific binding of [^{3}H]-brevenol should make it a very useful ligand in studying VSSCs in the plasma membrane of cells making up excitable tissues. Additionally, the isolation and localization of this novel brevenal/ol receptor, similar to those performed by Trainer and colleagues (1991, 1994) for the brevetoxin site, will provide more insight into the structure of VSSCs.

5. Conclusion

The presence of saturable, relatively high affinity binding that conforms to single-site statistical analysis as well as absence of binding inhibition by ligands that bind to other known sites fits the criteria for positing a new binding site on mammalian VSSC, the brevenal site. As brevenal has been shown to have positive therapeutic potential, the importance of having a brevenal site-specific radiolabeled ligand is obvious.

Acknowledgments

This work was supported by NIH grants PO1 ES10594-10 and the Ruth L Kirschstein National Research Service Award 5F31GM06900603. Portions of this article appear as part of the Doctoral dissertation of Elena P. Gold, UNC Wilmington.

References

Abraham WM, Bourdelais AJ, Sabater JR, Ahmed A, Lee TA, Serebriakov I, Baden DG. Airway responses to in an animal model. Am. J. Resp. Crit. Care Med. 2005; 171(1):26–34. [PubMed: 15447946]

Backer CB, Kirkpatrick B, Fleming LA, Cheung YS, Pierce R, Bean JA, Clark R, Johnson D, Wanner A, Tamer R, Zhou Y, Baden DG. Occupational exposure to aerosolized brevetoxins during Florida red tide events: Effects on a healthy worker population. Environ. Health Perspect. 2005; 113:644–649. [PubMed: 15866778]

Backer LC, Fleming LE, Rowan A, Cheng YS, Benson J, Pierce R, Zaias J, Bean JA, Bossart JD, Johnson D, Quimbo R, Baden DG. Recreational exposure to aerosolized brevetoxins during Florida red tide events. Harmful Algae. 2003; 2:19–28.

Baden DG. Marine food-borne dinoflagellate toxins. Int. Rev. Cytol. 1983; 82:99–150. [PubMed: 6352551]

Baden, DG.; Fleming, LE.; Bean, JA. Marine Toxins. In: deWolf, FA., editor. Handbook of Clinical Neurology: Intoxications of the Nervous System Part H. Natural Toxins and Drugs. Elsevier Press; Amsterdam: 1995. p. 141-175.

Baden DG, Mende TJ. Toxicity of 2 toxins from the Florida red tide marine dinoflagellate *Ptychodiscus brevis*. Toxicon. 1982; 20(2):457–462. [PubMed: 6896247]

Baden DG, Tomas CR. Variations in major toxin composition for six clones of *Ptychodiscus brevis*. Toxicon. 1988; 26(10):961–963. [PubMed: 3201483]

Bossart GD, Baden DG, Ewing RY, Roberts B, Wright SD. Brevetoxicosis in manatees (*Trichechus manatus latirostris*) from the 1996 epizootic: gross, histologic, and immunohistochemical features. Toxicol. Pathol. Mar-Apr;1998 26(2):276–82. [PubMed: 9547868]

Bourdelais AJ, Campbell S, Jacocks H, Naar J, Wright JLC, Carsi J, Baden DG. Brevenal is a natural inhibitor of brevetoxin action in sodium channel receptor binding assays. Cell. Mol. Neurobiol. 2004; 24(4):553–563. [PubMed: 15233378]

Cestele S, Catterall WA. Molecular mechanisms of neurotoxin action on voltage-gated sodium channels. Biochimie. 2000; 82(9-10):883–892. [PubMed: 11086218]

Dodd PR, Hardy JA, Oakley AE, Edwardson JA, Perry EK, Delaunoy JP. A rapid method for preparing synaptosomes comparison with alternative procedures. Brain Res. 1981; 226(1-2):107–108. [PubMed: 7296283]

Fleming LE, Kirkpatrick B, Backer LC, Bean JA, Wanner A, Dalpra D, Tamer R, Zaias J, Cheng YS, Pierce R, Naar J, Abraham W, Clark R, Zhou Y, Henry MS, Johnson D, Van de Bogart G, Bossart GD, Harrington M, Baden DG. Initial evaluation of the effects of aerosolized Florida red tide toxins (brevetoxins) in persons with asthma. Environ. Health Perspect. 2005; 113:652–657.

Fleming LE, Kirkpatrick B, Backer LC, Bean JA, Wanner A, Reich A, Zaias J, Cheng YS, Pierce R, Naar J, Abraham WM, Baden DG. Aerosolized red-tide toxins (brevetoxins) and asthma. Chest. 2007; 131:187–194. [PubMed: 17218574]

Flewelling LJ, Naar JP, Abbott JP, Baden DG, Barros NB, Bossart GD, Bottein MYD, Hammond DG, Haubold EM, Heil CA, Henry MS, Jacocks HM, Leighfield TA, Pierce RH, Pitchford TD, Rommel SA, Scott PS, Steindinger KA, Truby EW, Van Dolah FM, Landsberg JH. Red tides and marine mammal mortalities. Nature. 2005; 435:755–756. [PubMed: 15944690]

Kirkpatrick, B.; Hautamaki, R.; Kane, T.; Henry, M. A pilot study to explore the occupational exposure to *Gymnodinium* brevetoxin and pulmonary function. In: Hallegraeff, GM.; Bolch, CJ.; Blackburn, SI.; Lewis, RJ., editors. Harmful Algal Blooms; Proceedings of the 9th International Conference on Harmful Algal Blooms; Holbart, Tasmania. 7–11 February 2000; Paris: International Oceanographic Commission of UNESCO; 2001. p. 447-450.

LePage KT, Baden DG, Murray TF. Brevetoxin derivatives act as potential agonists at neurotoxin site 5 on the voltage gated Na^+ channel. Brain Res. 2003; 959:120–127. [PubMed: 12480165]

Lin YY, Risk M, Ray SM, Van Engen D, Clardy J, Golik J, James JC, Nakanishi K. Isolation and structure of brevetoxin B from the red tide dinoflagellate *Ptychodiscus brevis Gymnodinium breve*. J. Am. Chem. Soc. 1981; 103(22):6773–6775.

Mattei C, Molgo J, Legrand A-M, Benoit E. Ciguatoxins and brevetoxins: Dissection of their neurobiological actions. Journal de la Societe de Biologie. 1999; 193(3):329–344. [PubMed: 10542966]

Mattei C, Wen PJ, Nguyen-Huu TD, Alvarez M, Benoit E, Bourdelais AJ, Lewis RJ, Baden DG, Molga J, Meunier FA. Brevenal inhibits pacific ciguatoxin-1B-induced neurosecretion from bovine chromaffin cells. PLoS ONE. 2008; 3(10):e3448. [PubMed: 18941627]

Pierce RH, Henry MS, Blum PC, Lyons J, Cheng YS, Yazzie D, Zhou Y. Brevetoxin concentrations in marine aerosol: human exposure levels during a *Karenia brevis* harmful algal bloom. Bull. Environ. Contam. Toxicol. 2003; 70:161–165. [PubMed: 12478439]

Poli MA, Mende TJ, Baden DG. Brevetoxins unique activators of voltage-sensitive sodium channels bind to specific sites in rat brain synaptosomes. Mol. Pharm. 1986; 30(2):129–135.

Potera C. Marine and coastal science: Red tide chokehold. Environ. Health Perspect. 2007; 115:A188–A188. [PubMed: 17450197]

Purkerson-Parker SL, Fieber LA, Rein KS, Podona T, Baden DG. Brevetoxin derivatives that inhibit toxin activity. Chem. Bio. (London). 2000; 7(6):385–393.

Rein KS, Lynn B, Gawley RE, Baden DG. Brevetoxin B: Chemical modifications, synaptosome binding, toxicity, and an unexpected conformational effect. J. Org. Chem. 1994; 59(8):2107–2113.

Satake M, Bourdelais AJ, Van Wagoner RM, Baden DG, Wright JLC. Brevisamide: An unprecedented monocyclic ether alkaloid from the dinoflagellate *Karenia brevis* that provides a potential model for ladder-frame initiation. Org. Lett. 2008; 10:3465–3468. [PubMed: 18646771]

Satake M, Campbell A, Van Wagoner RM, Bourdelais AJ, Jacocks HM, Baden DG, Wright JLC. Brevisin: an aberrant polycyclic ether structure from the dinoflagellate *Karenia brevis* and its implications for polyether assembly. J. Org. Chem. 2009; 74:989–994. [PubMed: 19123836]

Segel, IH. Biochemical Calculations. 2nd Ed. John Wiley & Sons; New York, NY: 1968.

Steidinger, KA.; Baden, DG. Toxic marine dinoflagellates. In: Spector, DL., editor. Dinoflagellates. Academic Press; Orlando: 1984. p. 201-249.

Shimizu Y, Chou HN, Bando H, VanDuyne G, Clardy JC. Structure of brevetoxin A (gb-1), the most potent toxin in the Florida red tide organism (*Gymnodinium breve*). J. Am. Chem. Soc. 1986; 108:514–515. [PubMed: 22175476]

Shimizu, Y.; Gupta, S.; Prasad, AVK. Biosynthesis of dinoflagellate toxins. In: Graneli, E.; Sundstrom, B.; Edler, L.; Anderson, DM., editors. Toxic Marine Phytoplankton. Elsevier; New York: 1990. p. 62-76.

Trainer VL, Moreau E, Guedin D, Baden DG, Catterall WA. Neurotoxin binding and allosteric modulation at receptor sites 2 and 5 on purified and reconstituted rat brain sodium channels. J. Bio. Chem. 1993; 268(23):17114–17119. [PubMed: 8394327]

Truxal LT, Bourdelais AJ, Jacocks HM, Abraham WA, Baden DG. Characterization of Tamulamides A and B: Polyethers isolated from the marine dinoflagellate *Karenia brevis*. J. Nat. Prod. 2010; 73(4):536–540. [PubMed: 20218657]

Highlights

- Brevenal competes with brevetoxin for binding at site 5
- A new radiolabeled ligand [^{3}H]-brevenol was produced
- Brevetoxin cannot inhibit binding of [^{3}H]-brevenol
- Ligands selective for other sites do not inhibit [^{3}H]-brevenol binding
- Brevenal binds to a previously unreported site

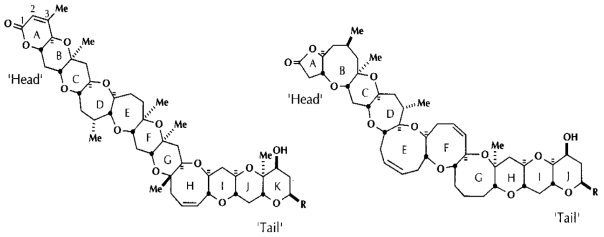

Brevetoxin B backbone:
PbTx-2, R=$CH_2C(=CH_2)CHO$
PbTx-3, R=$CH_2C(=CH_2)CH_2OH$
PbTx-5, [PbTx-2], C-37 O Ac
PbTx-6, [PbTx-2], C27, 28 Epoxide
PbTx-8, R=CH_2COCH_2Cl
PbTx-9, R=$CH_2CH(CH_3)CH_2OH$

Brevetoxin A backbone:
PbTx-1, R=$CH_2C(=CH_2)CHO$
PbTx-7, R=$CH_2C(=CH_2)CH_2OH$
PbTx-10, R=$CH_2CH(CH_3)CH_2OH$

Figure 1.
Structure of all published brevetoxins (PbTxs) (Rein *et al.* 1994).

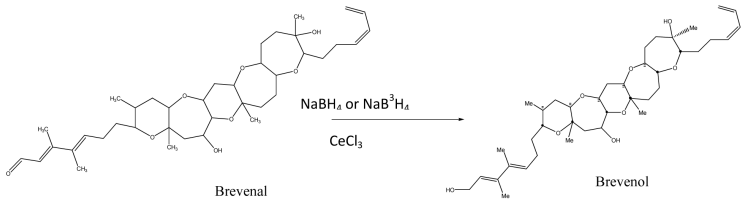

Figure 2.
Structure of brevenal and synthesis brevenol and [^{3}H]-brevenol.

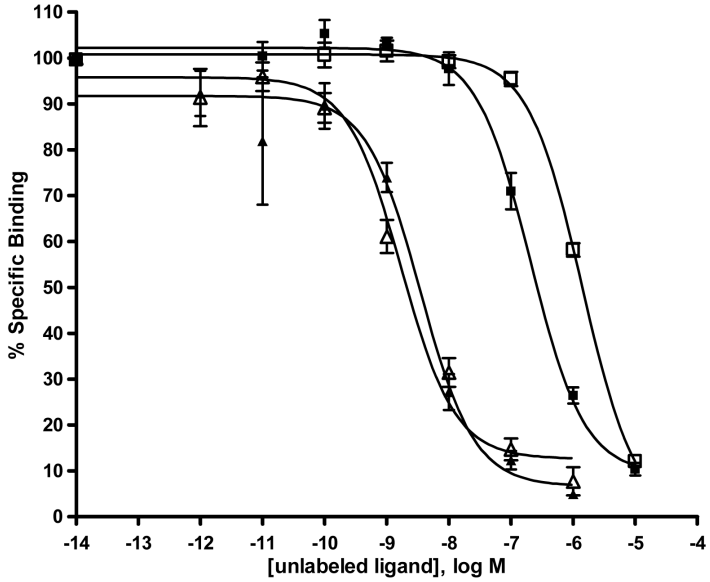

Figure 3.

Reduction of ^{3}H-PbTx-3 binding as a percent of the maximum specific binding using unlabeled competitors: (▵) PbTx-2, (▲) PbTx-3, (■) brevenal, and (□) brevenol. Each data point represents the mean ± s.e.m. of values obtained from three independent experiments with triplicate determinations in each experiment. Nonspecific binding was 20% of the total binding.

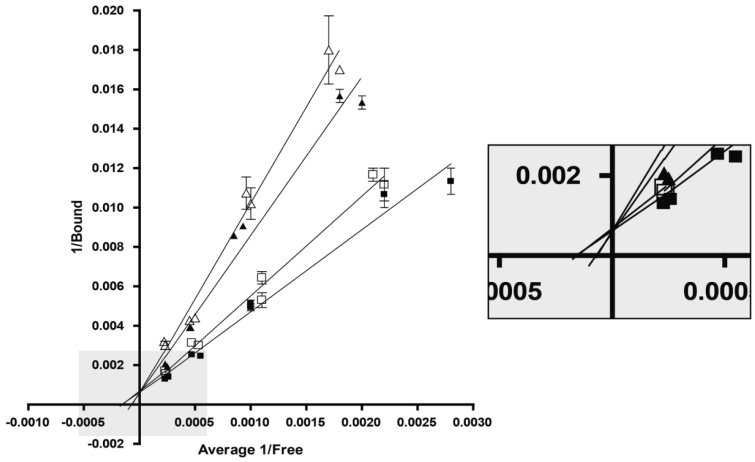

Figure 4.

Competitive inhibition of ^{3}H-PbTx-3 binding to site 5 (VSSC) by brevenol. Synaptosomes were incubated for 1 hour at 4°C with increasing concentrations of ^{3}H-PbTx-3 in the presence of (■) 0 nM, (□) 10 nM, (▲) 25 nM, or (▵) 50 nM brevenol. Each point represents the mean ± s.e.m. of values obtained from two independent experiments with triplicate determinations per experiment.

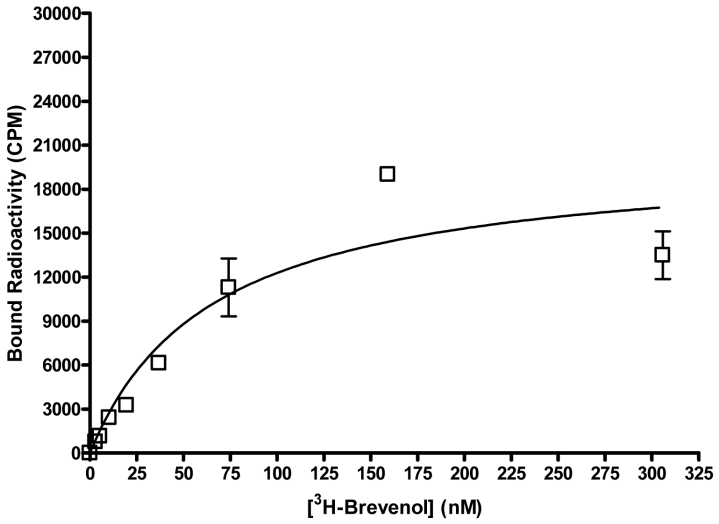

Figure 5.

(A) Specific[1] saturation binding of ^{3}H-brevenol to rat brain synaptosomes. Each data point represents the mean ± s.e.m. of triplicate determinations for each concentration. Analysis of nonlinear regression of specific binding yields an approximate K_D of 67.5 nM and a B_{max} of 7.2 ± 0.9 pmoles of ^{3}H-brevenol per mg of synaptosomal protein.

[1] Total and nonspecific binding were measured by liquid scintillation techniques, the difference between the two represent specific (□) binding.

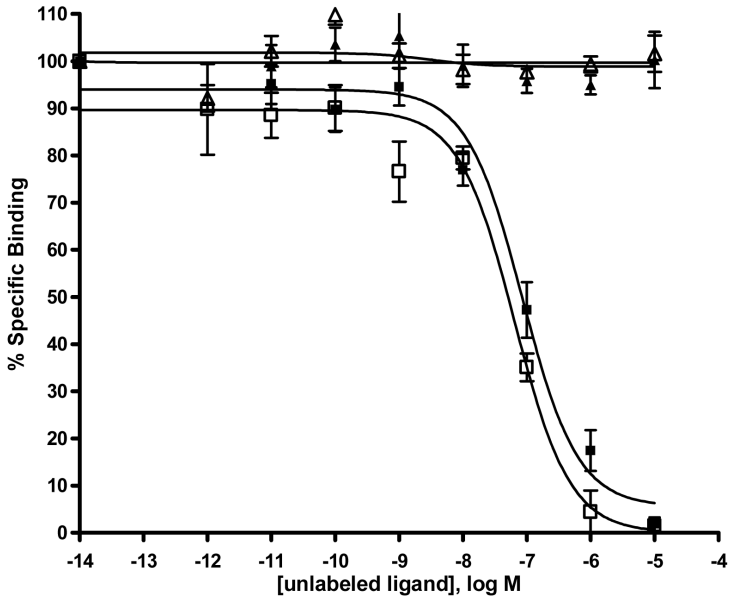

Figure 6.

Reduction of ^{3}H-brevenol binding as a percent of the maximum specific binding using unlabeled competitors: (▵) PbTx-2 (site 5), (▲) PbTx-3 (site 5), (■) brevenal, and (□) brevenol. Each data point represents the mean ± s.e.m. of values obtained from three independent experiments with triplicate determinations in each experiment. Nonspecific binding was calculated as 20% of the total binding.

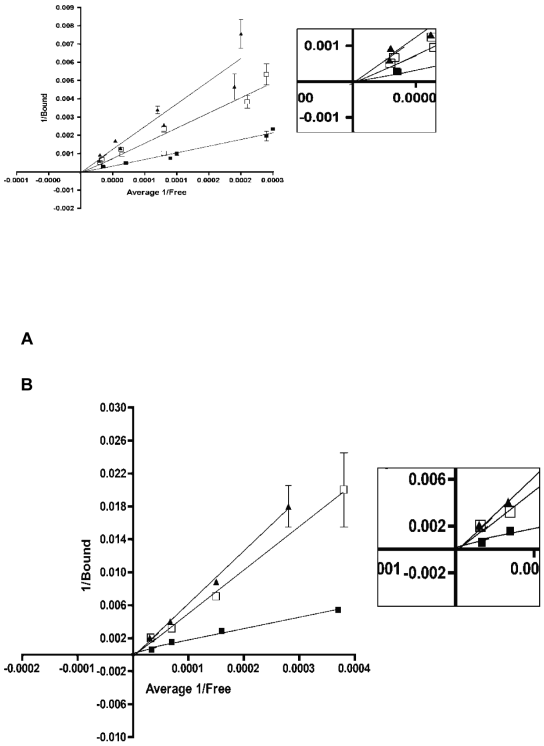

Figure 7.

A. Competitive Inhibition of ^{3}H-brevenol versus brevenol. Synaptosomes were incubated for 1 hour at 4°C with increasing concentrations of ^{3}H-brevenol in the presence of (■) 0 nM, (□) 10 nM, or (▲) 25 nM brevenol. Each data point represents the mean ± s.e.m. of values obtained from three independent experiments with triplicate determinations in each experiment. B. Competitive Inhibition of ^{3}H-brevenol by brevenal. Synaptosomes were incubated with increasing concentrations of ^{3}H-brevenol in the presence of (■) 0 nM, (□) 10 nM, or (▲) 25 nM brevenal. Each data point represents the mean ± s.e.m. of values obtained from three independent experiments with triplicate determinations in each experiment.

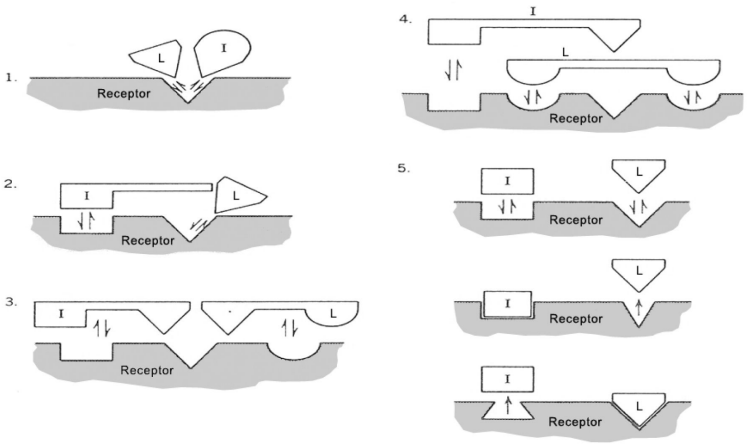

Figure 8.
(adapted from Segel 1968). Interactions between cell surface receptors, ligands (L) and inhibitors (I). These interactions are used to explain the binding of PbTxs to site 5 and the novel brevenal/ol receptor located on VSSCs.

Table 1

Inhibition of [^{3}H]-brevenol binding by site-selective ligands

Ligands	Inhibition of [^{3}H]-brevenol binding (maximum concentration tested)	Receptor site on VSSC/VGSC
Tetrodotoxin	No displacement (10 ! M)	Site 1
Veratridine or aconitine	No displacement (10 ! M)	Site 2
Leiurus quinquestriatus venom	No displacement (50 ! g/mL)	Site 3
Centruroides sculpturatus venom	No displacement (50 ! g/mL)	Site 4
Brevetoxins 2 & 3	No displacement (10 ! M)	Site 5
Amiloride	No displacement (10 ! M)	Blocks sodium channels
Deltamethrin	No displacement (100 ! M)	Pyrethroid site
Brevenal	K_i=74.8 nM	(new)
Brevenol	K_i=56.5 nM	(new)